

## Kinematic modeling and accuracy analysis of the pyramidal delta robot

S.Houmairi<sup>1</sup>, Y.Kardaboussi<sup>2</sup>, B. Elhadim<sup>3</sup>, N. Boumaaz<sup>4</sup>

<sup>1</sup> Educational training center CRMEF Casa-Settat, Morocco. E-mail: *houmairi.said50@gmail.com*

<sup>2</sup> EMINES School of Industrial Management-UM6P, BenGuerir, Morocco

<sup>3</sup> Educational training center CRMEF Casa-Settat, Morocco

<sup>4</sup> Higher School of Technology EST, Safi, Morocco

### Abstract:

This article presents an original work about the development of a low-cost 3D printer based on the pyramidal delta robot. First, this architecture's kinematic modeling is presented. Second, the ideal design parameter dimensions are synthesized using a geometrical approach. Third, a method for accuracy analysis inside the workspace is suggested. Numerical results demonstrate the potential of this architecture for the development of low-cost 3D printers. The kinematic modeling and the accuracy analysis are useful for design and comparison of the delta robots based 3D printers.

**Keywords:** -delta robot, accuracy analysis, forward kinematic, inverse kinematic, pyramidal delta robot.

### 1. Introduction:

For the past three decades, delta robots have remained the most commercially successful models from parallel architecture. The first model was invented by ReymondClevel [1, 2, 3]. The basic three degrees of freedom of the linear delta robot are formed by two platforms connected through three identical kinematic chains, where one of the platforms is usually defined as mobile. Each kinematic chain is constituted by links parallelogram with spherical joints. This kind of architectures exhibit very good performances in terms of high speed, low inertia, good stiffness and accuracy. [4], [5], [6], [7], [8]. Despite all these benefits, a short coming of linear delta robots is their limited workspace. [9].

For most applications, and especially in 3D printer cases, positioning accuracy is one of the most important design requirements [10]. Therefore, simple and fast methods for computing the accuracy of a given robot design are needed in order to use them in design optimization procedures that look for maximum accuracy. [11].

Errors in the position and orientation of a parallel robot are due to several factors: Manufacturing, compliance, active joint errors and so forth. As pointed out by Merlet [12], active-joint errors (input errors) are the most significant source of errors in a properly designed, manufactured, and calibrated parallel robot. Performance indices and accuracy has been extensively studied and various accuracy indices have been defined such as condition number, manipulability, Isotropy and global conditioning index [13]. For delta robot, the most appropriate accuracy index is the maximal positioning errors [14].

In this work, a novel delta robot configuration is investigated. In this arrangement, the linear guide axes are angled to form a pyramid. The proposed study shows the potential of this pyramidal configuration for the development of a low cost 3D printer.

This paper is organized as follows: Section 2 presents a kinematic modeling of the pyramidal delta robot. A geometric method to synthesize the primary parameter dimensions for a desired workspace is presented in Section 3. Accuracy analysis inside the workspace is then performed in section 4. Section 5 shows a numerical result. Finally, the study is concluded in Section 6.

## 2. Kinematic modeling of pyramidal delta robot

As illustrated in figure 1, the pyramidal Delta robot has three translational degrees of freedom and is made up of a fixed platform and a moving platform coupled by three similar kinematic chains. The actuating sub-system is housed on the fixed platform, while the end-effector is housed on the moving platform.

Geometric centers of the fixed and moving platforms are denoted by points  $O$  and  $O'$  respectively. The coordinate system  $O$ -xyz is assumed to be at the geometric center of the fixed platform with the  $z$ -axis normal to the base and the  $y$ -axis directed along  $A_3O$ .

The center of the link for each of the three chains connected to the pyramidal base is denoted as  $B_i$  ( $i= 1, 2, 3$ ), and the center of the interval between the two spherical joints connecting the moving platform in each chain is denoted as  $P_i$  ( $i= 1, 2, 3$ ).

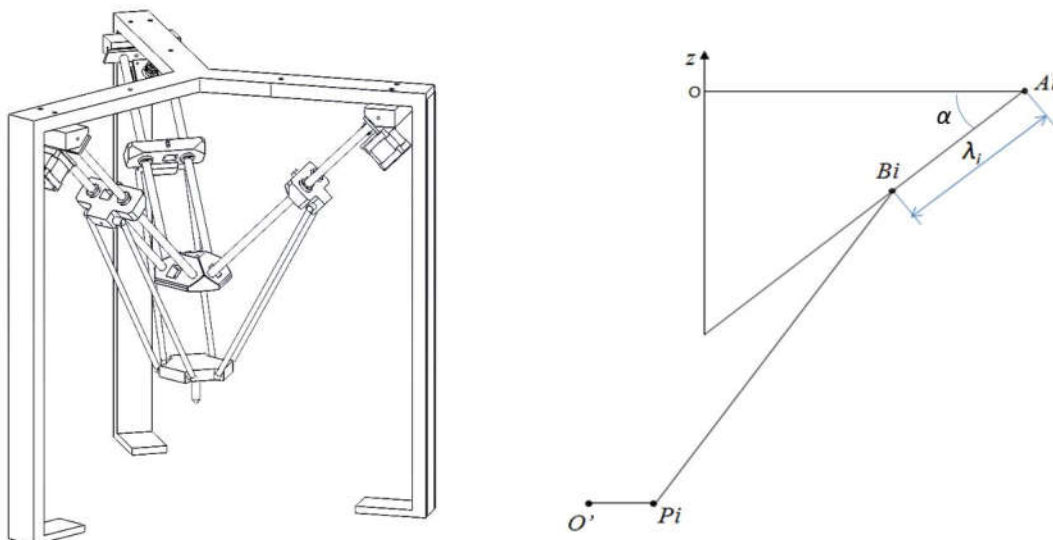


Fig. 1: (a) CAD model of the pyramidal Delta robot; (b) kinematic description of the  $i^{th}$  kinematic chain

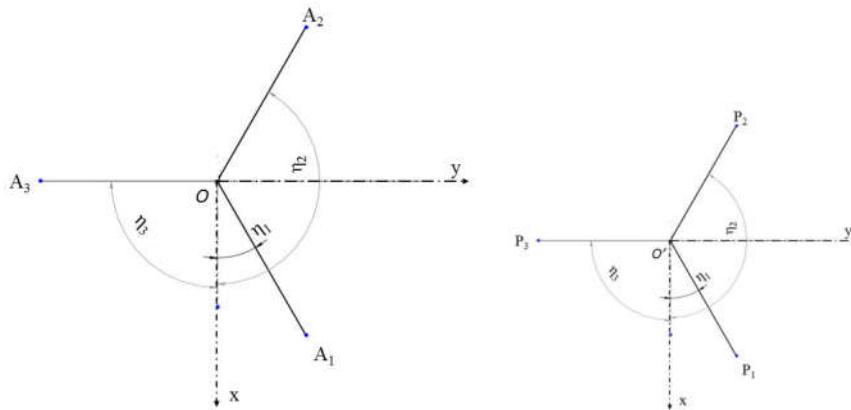


Figure 2: Top view of the base and the moving platform.

Suppose that the radii of the base and the moving platform are  $R$  and  $r$  respectively, ie.  $OA_i = R$ ,  $O'P_i = r$ . The length of the parallelogram joint is equal to  $L$ . Then  $\eta_i = \frac{4i-3}{6}\pi$  denote the angle from  $x$  axis to line  $OA_i$ .

**2.1. Inverse Position kinematic (IPK)**

The goal of inverse kinematics is to find the robot's inputs that correspond to the given reference point position  $O'$ . Taking a kinematic chain as an example, according to the geometric method, the closed-loop equation of the  $i$ th chain is:

$$\overrightarrow{OA_i} + \overrightarrow{A_iB_i} + \overrightarrow{B_iP_i} + \overrightarrow{P_iO'} + \overrightarrow{O'O} = \vec{0} \quad (1)$$

The coordinate of the point  $O'$  in the moving platform can be written as  $\overrightarrow{OO'} = (x, y, z)^T$ . And  $\overrightarrow{A_iB_i} = (-\lambda_i \cos \varphi \cos \eta_i, -\lambda_i \cos \varphi \sin \eta_i, -\lambda_i \sin \varphi)^T$  denote the actuated joints variables. The vectors  $\overrightarrow{OA_i}$  and  $\overrightarrow{P_iO'}$  can be respectively expressed in coordinate system  $0$ - $xyz$  as  $\overrightarrow{OA_i} = (R \cos \eta_i, R \sin \eta_i, 0)^T$ ,  $\overrightarrow{P_iO'} = (-r \cos \eta_i, r \sin \eta_i, 0)^T$ .

The inverse kinematics of the Delta robot can be solved by writing following constraint equations:  $(\overrightarrow{B_iP_i})^2 = L^2$ . Then the vector equation (1) is converted into three scalar equations, yielding:

$$L^2 = [x - (R - r) \cos \eta_i + \lambda_i \cos(\varphi) \cos(\eta_i)]^2 + [y - (R - r) \cos \eta_i + \lambda_i \cos(\varphi) \sin(\eta_i)]^2 + [z + [\lambda_i \sin(\varphi)]]^2 \quad (2)$$

Where  $\eta_i = \frac{4i-3}{6}\pi$ , and  $i = 1, 2, 3$ .

The three scalar equations can then be written as follows:

$$\lambda_1^2 + B_1 \lambda_1 + C_1 = 0 \quad (3)$$

$$\lambda_2^2 + B_2 \lambda_2 + C_2 = 0 \quad (4)$$

$$\lambda_3^2 + B_3 \lambda_3 + C_3 = 0 \quad (5)$$

Where:

$$B_1 = -\sqrt{2}(R-r) + \frac{\sqrt{6}}{2}x + \frac{\sqrt{2}}{2}y + \sqrt{2}z$$

$$B_2 = -\sqrt{2}(R-r) - \frac{\sqrt{6}}{2}x + \frac{\sqrt{2}}{2}y + \sqrt{2}z$$

$$B_3 = -\sqrt{2}(R-r) - \sqrt{2}y + \sqrt{2}z$$

$$C_1 = x^2 + y^2 + z^2 - L^2 + (R-r)^2 - \sqrt{3}x(R-r) - y(R-r)$$

$$C_2 = x^2 + y^2 + z^2 - L^2 + (R-r)^2 + \sqrt{3}x(R-r) - y(R-r)$$

$$C_3 = x^2 + y^2 + z^2 - L^2 + (R-r)^2 + 2y(R-r)$$

Solving the three quadratic equations (3), (4), and (5) yields the following result:

$$\lambda_1 = \frac{-B_1 - \sqrt{\Delta_1}}{2}; \lambda_2 = \frac{-B_2 - \sqrt{\Delta_2}}{2}; \lambda_3 = \frac{-B_3 - \sqrt{\Delta_3}}{2}$$

Where:  $\Delta_i = B_i^2 - 4C_i$

It is worth noting that the problem has two solutions for each lambda. However, due to the robot's configuration, only one solution is considered.

## 2.2. Forward Position kinematic (FPK):

The goal of forward kinematics is to determine the pose of the end effector  $x, y$  and  $z$  in relation to the coordinates of the actuated joints  $\lambda_i$ .

The forward kinematic solution begins with the three scalar equations (2). By subtracting the second equation from the first, and the third from the first, we obtain two algebraic equations relating the coordinates  $x, y$  and  $z$ .

$$a_1x + b_1y + c_1z + d_1 = 0 \quad (6)$$

$$a_2x + b_2y + c_2z + d_2 = 0 \quad (7)$$

Where:

$$a_1 = \frac{\sqrt{6}}{2}(\lambda_1 + \lambda_2) - 2\sqrt{3}(R-r)$$

$$b_1 = \frac{\sqrt{2}}{2}(\lambda_1 - \lambda_2)$$

$$c_1 = \sqrt{2}(\lambda_1 - \lambda_2)$$

$$d_1 = \lambda_1^2 - \lambda_2^2 - \sqrt{2}(R-r)(\lambda_1 - \lambda_2)$$

$$a_2 = \frac{\sqrt{6}}{2}\lambda_1 - \sqrt{3}(R-r)$$

$$b_2 = \frac{\sqrt{2}}{2}\lambda_1 + \sqrt{2}\lambda_3 - 3(R-r)$$

$$c_2 = \sqrt{2}(\lambda_1 - \lambda_3)$$

$$d_2 = \lambda_1^2 - \lambda_3^2 - \sqrt{2}(R - r)(\lambda_1 - \lambda_3)$$

From the two algebraic equations (6) and (7), the coordinates  $x$  and  $y$  can be expressed in terms of  $z$  only. Then:

$$x = Az + B \quad (8)$$

$$y = Ez + F \quad (9)$$

Where:

$$A = \frac{-(c_1 - c_2 \frac{b_1}{b_2})}{(a_1 - a_2 \frac{b_1}{b_2})}$$

$$B = \frac{-(d_1 - d_2 \frac{b_1}{b_2})}{(a_1 - a_2 \frac{b_1}{b_2})}$$

$$E = \frac{-(c_1 - c_2 \frac{a_1}{a_2})}{(b_1 - b_2 \frac{a_1}{a_2})}$$

$$F = \frac{-(d_1 - d_2 \frac{a_1}{a_2})}{(b_1 - b_2 \frac{a_1}{a_2})}$$

The substitution of the expressions of  $x$  and  $y$  in one of the equations (2), leads to a quadratic equation:

$$\alpha z^2 + \beta z + \gamma = 0$$

Where:

$$\alpha = A^2 + E^2 + 1$$

$$\beta = 2AB + 2EF + Aa_2 + E \left( \frac{\sqrt{2}}{2} \lambda_1 - (R - r) \right) + \sqrt{2} \lambda_1$$

$$\gamma = B^2 + F^2 + Ba_2 + F \left( \frac{\sqrt{2}}{2} \lambda_1 - (R - r) \right) + (R - r)^2 - L^2 + \lambda_1^2 - \sqrt{2} \lambda_1 (R - r)$$

The solution is as follows:

$$z = \frac{-\beta - \sqrt{\Delta}}{2\alpha}$$

Where  $\Delta = \beta^2 - 4\alpha\gamma$ .

It's worth noting that only one solution is considered due to the robot's configuration in figure 1.

### 3. Optimal design

The optimal robot designs take into account various indices to determine the platform radius  $R$ ,  $r$ , and link length  $L$ . The procedure is a complicated program that must take into account a variety of factors, including workspace, the conditioning index, singularity, application, and so forth [15].

This section examines the design in terms of the desired workspace, which is a cylindrical volume with a radius denoted by  $r_0$  and a height denoted by  $H_0$ . The suggested approach makes it

easy to choose the robot's ideal dimensions so that it can move through the entire desired workspace. However, some dimensions need to be set up in advance. These parameters are affected by operating or design restrictions. These constraints can be explained as follows:

- The minimal value of the parameter  $R_l$  can be fixed according to the wide of linear guide.
- The  $\psi$  angle cannot exceed the  $\alpha$  angle due to interference with linear guides
- To prevent interference between the ball joints, the mobile platform's minimum radius  $r_{min}$  is constrained by the width of the parallelograms formed by the links.

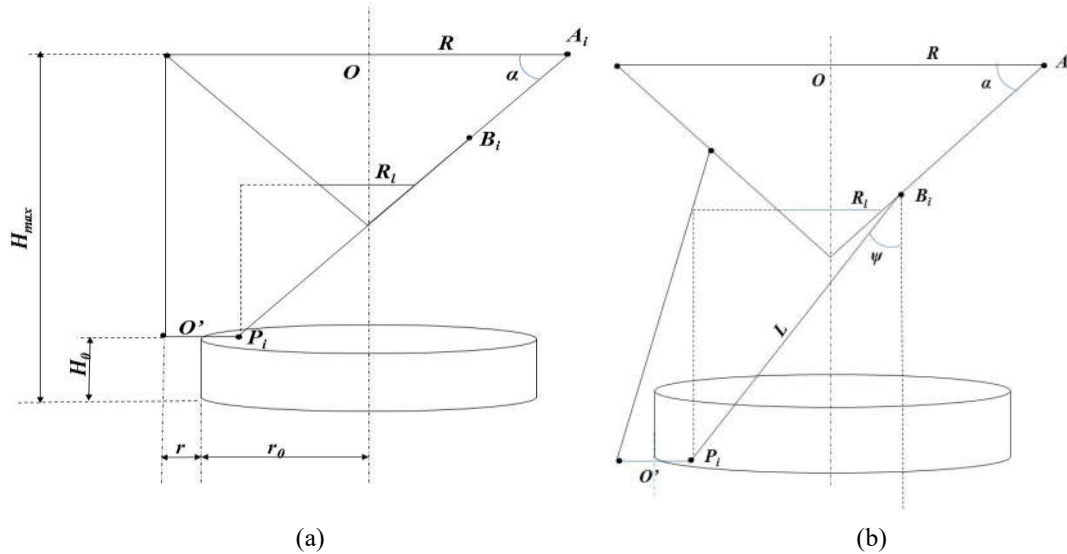


Fig. 3 :Extrem positions of the mobile platform in the cylindrical workspace

As shown in figure (3 a), the moving platform is assumed to be at the plane  $z=H_0$ , and the reference point  $O'$  is assumed to extend to the workspace's furthest point. At these pose, there are:

$$R - r = r_0 \quad (10)$$

$$L_{max} = 2R - 2r \quad (11)$$

In the figure (3 b), the moving platform is assumed to be at the plane  $z=0$ , and the reference point  $O'$  is assumed to extend to the workspace's furthest point. At these pose, there are:

$$\text{tang}(\psi) = \frac{R-2r+R_l}{L_{max}-R+R_l} \quad (12)$$

$$L_{min} \sin(\psi) = R - 2r + R_l \quad (13)$$

For the proposed studies, the fixed parameters are:  $R_l=40\text{mm}$ ,  $r=40\text{mm}$ . All others parameters depicted in table I are determined using the equations (10) (11) (12) and (13).

Table I: Dimensions of delta robot

Parameters	Value [mm]
$\psi_{max}$	$45^\circ$
$R$	40
$R_l$	40

$R$	190
$L_{max}$	300
$L_{min}$	225

#### 4. Accuracy analysis

The positioning error of a robot is defined as the smallest incremental move that the robot can physically produce. A practical definition of the resolution can be expressed as [13]

$$E = \sqrt{\delta x^2 + \delta y^2 + \delta z^2}$$

Where  $\delta x$ ,  $\delta y$ ,  $\delta z$  represent the smallest displacements that the mobile platform can perform for smallest movement of the motor step. Hence,  $\delta x$ ,  $\delta y$ ,  $\delta z$  can be defined as:

$$\begin{aligned}\delta x &= \frac{\partial x}{\partial \lambda_1} d\lambda_1 + \frac{\partial x}{\partial \lambda_2} d\lambda_2 + \frac{\partial x}{\partial \lambda_3} d\lambda_3 \\ \delta y &= \frac{\partial y}{\partial \lambda_1} d\lambda_1 + \frac{\partial y}{\partial \lambda_2} d\lambda_2 + \frac{\partial y}{\partial \lambda_3} d\lambda_3 \\ \delta z &= \frac{\partial z}{\partial \lambda_1} d\lambda_1 + \frac{\partial z}{\partial \lambda_2} d\lambda_2 + \frac{\partial z}{\partial \lambda_3} d\lambda_3\end{aligned}$$

Where  $\frac{\partial x}{\partial \lambda_i}$  represent the partial derivative of  $x$  with respect to  $\lambda_i$ .

Analytical resolution of the problem is very fastidious. In this work, the partial derivatives are performed using the symbolic tool of Python programming language. The resulting formulas are very lengthy, so one feasible method is to enter the resulting expressions into the Julia programming language and run the numerical calculus using the following algorithm:

Algorithm 1:

Inputs:

- Design parameter variable:  $R$ ,  $r$ ,  $L$ .
- Coordinate of investigated plane:  $z$
- Size of reachable workspace:  $x_{min}, x_{max}, y_{min}, y_{max}$ .
- The sampling space step:  $step_x$ ,  $step_y$

Find:

- Local error  $E$  about  $(O', x, y, z)$
1.  $[x, y] = \text{meshgrid}(x_{min} : step_x : x_{max}, y_{min} : step_y : y_{max})$
  2.  $[\lambda_1, \lambda_2, \lambda_3]^T = \text{IPK}(x, y, z, R, r, L)$
  3. For  $i=1:\text{length}(x)$
  4. For  $j=1:\text{length}(y)$
  5.  $\delta x(i, j)$ ,  $\delta y(i, j)$  and  $\delta z(i, j)$  (are calculated from the symbolic expression of the partial derivative).
  6.  $E(i, j) = \sqrt{\delta x(i, j)^2 + \delta y(i, j)^2 + \delta z(i, j)^2}$
  7. End  $j$

8. End i

**5. Numerical result:**

This section presents a numerical validation of the IPK and FPK equations, the FPK equations are then used to numerically determine the reachable workspace. In order to support the selection of the actuator, the resolution of the accessible workspace is examined last.

**5.1. IPK and FPK validation**

The moving platform control point O' is intended to trace an 80 mm-diameter circle with a center located at (0,0,-350)T. Figure 4 displays this hypothetical trajectory. The IPK equation is then used to compute the active joint coordinates  $\lambda_i$  as mentioned in section 2.1. To get the calculated trajectory, the FPK equations are then applied. As shown in figure 6, the calculated trajectory is exactly similar to the simulated one.

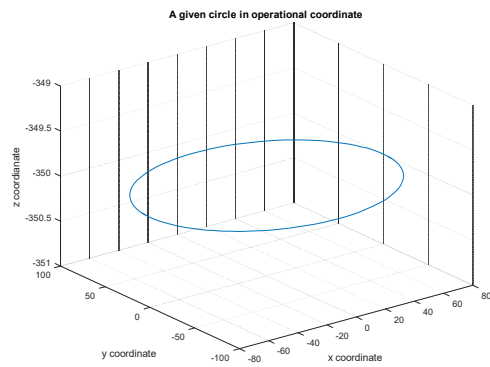


Fig 4. Simulated trajectory in  $\theta$ -xyz Coordinate.

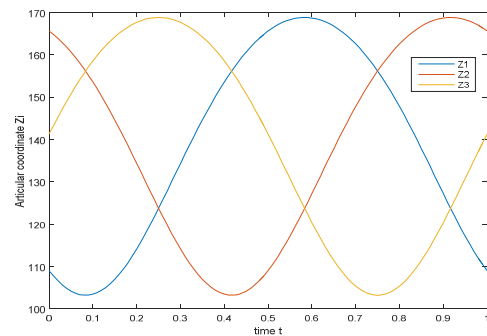


Fig.5. Active joint coordinate  $\lambda_i$  using IPK equations.

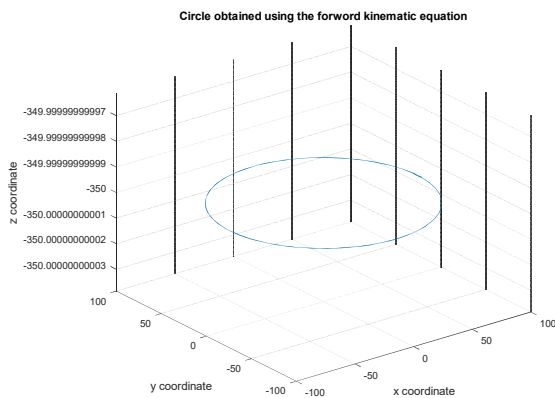


Fig.6. Calculated trajectory using FPK equations

**5.2. Reachable workspace**

The reachable workspace represents the area covered by the delta robot when some of the parameter is varied such as active joint or link length [16]. The method considered in this work is based on forward kinematic. Figure 7 shows the theoretical reachable pose of the reference point of the mobile platform O', when the actuated joint parameters  $\lambda_i$  vary from 0 to 212 mm with step equal to 10 mm. This study aims to validate the proposed prototype in term of inscribed



cylindrical workspace. Figure 8 illustrate the inscribed cylinder and the reachable workspace profile.

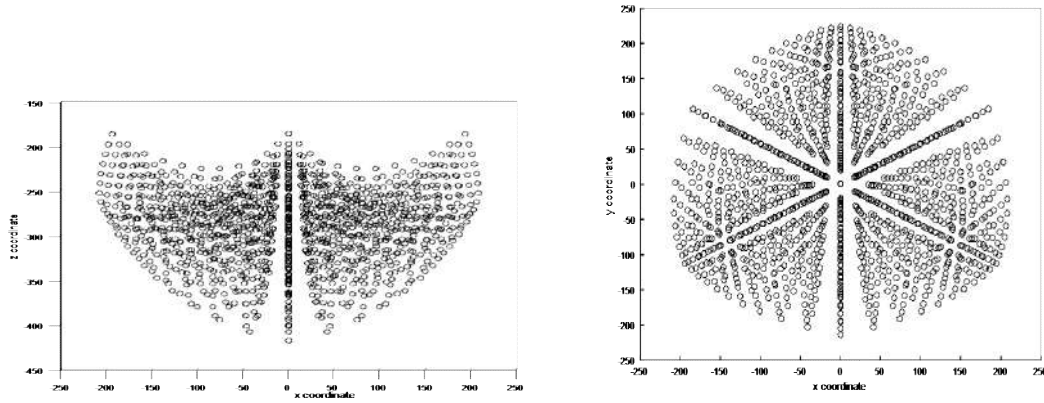


Fig.7.(a) Reachable workspace Profile. (b): Top view of Reachable workspace

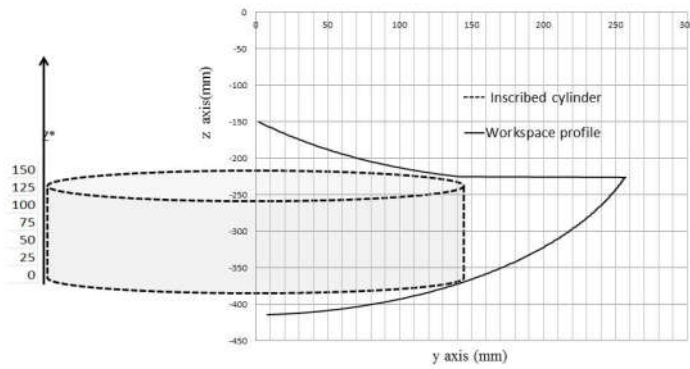
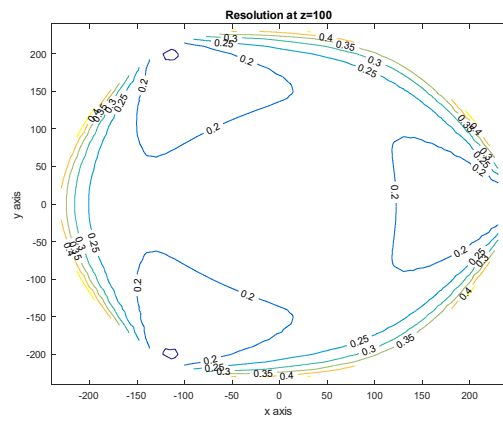
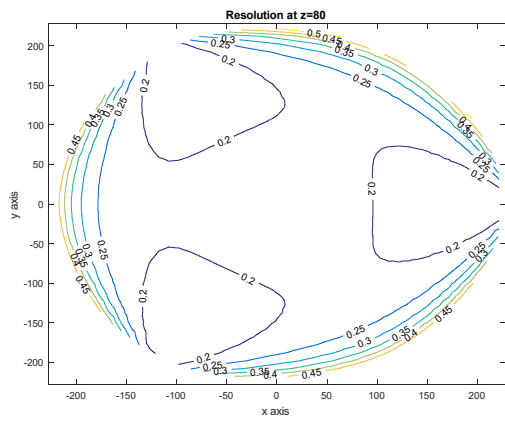
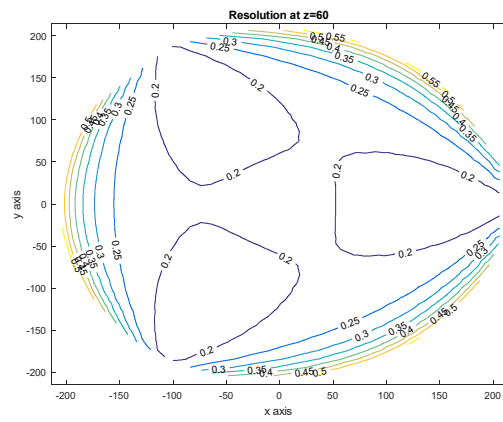
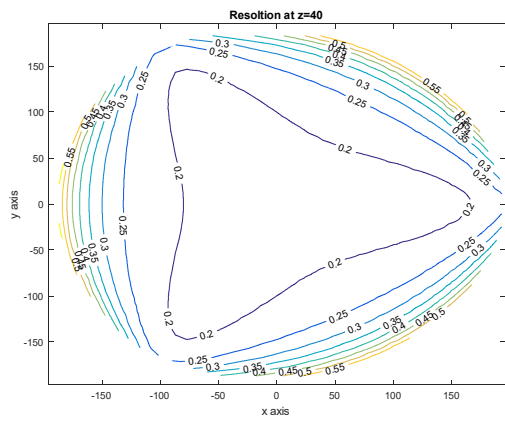
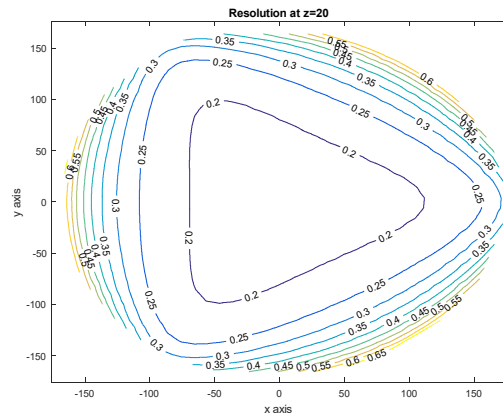
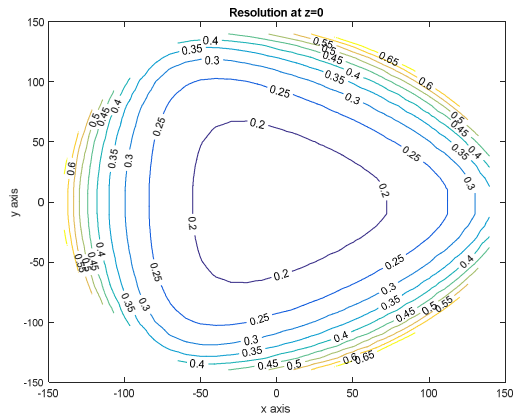


Fig.8. Position of the inscribed cylinder in the reachable workspace profile

### 5.3. Accuracy inside the reachable workspace

Accuracy analysis is done by visualizing the error  $E$ , defined in section 4, across a plane inside the reachable workspace of the Delta robot. The investigated planes are discretized with a given density along  $x$  and  $y$  axis. And the local positioning error is calculated at each point using the algorithm presented in section 4.



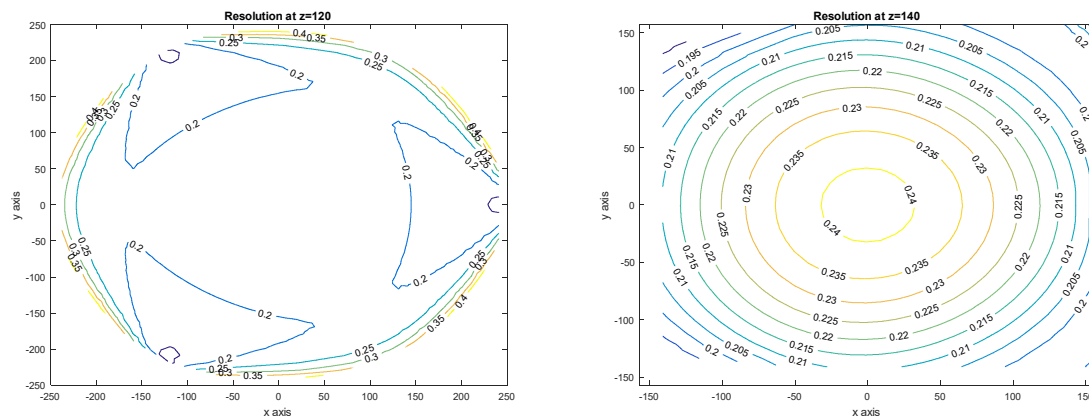


Fig.8. Local error across planes (x,y).z varies from 0 to 140 mm with step=20mm

The actuator step considered in this simulation is 1.8 degrees. As illustrated in figure 8, the positioning error in the inscribed cylinder is about 0.25 mm, and orientated in the same way as the three active joints around the axis(O,z). For 3D printing applications based on extrusion of constant filament, this result is sufficient, but for more accuracy, it is suitable to use a 0.9 degree stepper.

## 6. Conclusion

In this article, an original study of the pyramidal delta robot is presented. This study concerns kinematic modeling, optimal dimensions and accuracy analysis inside the reachable workspace. The study shows that the suggested model offers a wide and flat workspace. The resolution analysis indicates that a typical stepper motor can be used as an actuator. The produced prototype yields a successful outcome. Future research will focus on calibration techniques to increase accuracy.

## References:

- [1] R.Clavel:**Device for the movement and positioning of an element in space**  
Dec. 11 1990, US Patent 4,976,582.
- [2] R.Clavel. **A fast robot with parallel geometry**  
Int. Symposium on Industrial Robots, (1988), pp. 90–100.
- [3] Alberto J. Alvares, Efraín A. R. Gasca, Cristhian I. R. Jaimes, **Development of the linear delta robot for additive manufacturing**  
5th International Conference on Control, Decision and Information Technologies, Thessaloniki, Greece, April 10-13, (2018).<https://doi.org/10.1109/CoDIT.2018.8394869>.
- [4], M. I.Dawood, V. Kavati.**Design and Analysis of 3 - Axis Delta Type Parallel Robot**  
High Technology Letters, Volume 26, Issue 10, 2020.
- [5]Lou, Y., Lu, G, Xu, J., and Li, Z. **A general approach for optimal kinematic design of parallel manipulators**  
Proc IEEE Int. Conf. Robot.Auto, New Orleans, (2004), pp.3659-3664.<https://doi.org/10.1109/ROBOT.2004.1308827>.
- [6] Lou, Y., Liu, G., Chen, N., and Li, Z.**Optimal design of parallel manipulators for maximum effective regular workspace**

- Proc. IEEE/RSJ Int. Conf. on Intel. Robots Sys., Alberta, (2005), pp.795–800. <https://doi.org/10.1109/IROS.2005.1545144>.
- [7] M. López, E. Castillo, G. García, A. Bashir 2006. **Delta robot: Inverse, direct, and intermediate Jacobians**  
P. I. Mech. Eng. C J. Mec., (2006), 220, 103–109. DOI: 10.1243/095440606X78263.
- [8] J.-P. Merlet 2006. **Parallel Robots**, Springer Science & Business Media, 2006.
- [9] César M. A. Vasques, and Fernando A. V. Figueiredo, **The 3D-Printed Low-Cost Delta Robot Óscar: Technology Overview and Benchmarking**  
Eng. Proc., (2021), 11, 43. <https://doi.org/10.3390/ASEC2021-11173>.
- [10] Yu Li, Deyong Shang and Yue Liu, **Kinematic modeling and error analysis of Delta robot considering parallelism error**  
International Journal of Advanced Robotic Systems, (2019), 1–9. <https://doi.org/10.1177%2F1729881419878927>.
- [11] Sébastien Briot, Ilian Bonev. **Accuracy Analysis of 3-DOF Planar Parallel Robots**, Mechanism and Machine Theory, Elsevier, (2008), 43 (4), pp.445–458. <https://doi.org/10.1016/j.mechmachtheory.2007.04.002>.
- [12] J.-P. Merlet. **Computing the worst case accuracy of a PKM over a workspace or a trajectory**  
The 5th Parallel Kinematics Seminar, Chemnitz, Germany, (2006), pp. 83–96.
- [13] Mansoor Ghazi. **Accuracy analysis of 3-RSS delta parallel manipulator**  
Procedia Manufacturing 17 (2018) 174–182, Columbus, OH, USA. <https://doi.org/10.1016/j.promfg.2018.10.033>.
- [14] Jean-Pierre Merlet. **Jacobian, manipulability, condition number and accuracy of parallel robots**  
ISRR, (2005), San Francisco. inria-00000001v1. <https://doi.org/10.1115/1.2121740>
- [15] Xin-Jun Liu, Jinsong Wang, Kun-Ku Oh and Jongwong Kim. **A New Approach to the Design of a DELTA Robot with a Desired Workspace**  
Journal of Intelligent and Robotic Systems, (2004), 39: 209–225. <https://doi.org/10.1023/B:JINT.0000015403.67717.68>.
- [16] Aziah Khamis, Nor Aishah Muhammad, and Nur Syafiqah Zulfakar, **Workspace Analysis and Development of Delta Robot Using Forward Kinematic**  
International Journal of Mechanical & Mechatronics Engineering IJMME-IJENS, (2020), Vol:20 No:06.